To appear in:

Journal of Theoretical and Applied Physics

Online ISSN: 2251-7235 **Print ISSN: 2251-7227**

Received: 30 January 2026

Revised: 30 March 2026

Accepted: 08 May 2026

DOI: https://doi.org/10.57647/jtap.2026.2005.06

Research Article

Investigation of Renal Failure Impact on Blood Mineral Equilibrium Employing Laser Spectroscopy

Noor Hameed Nasif[1], Bahaa Jawad Alwan[2*], Nedaa Monther Salman[3], Sarah Mahmoud Abdallh[4]

[1.4]Department of Physics, College of Science, University of Diyala, Diyala, Iraq
[2]Department of Physics, College of Science, Mustansiriyah University, Baghdad, Iraq
[3]Open Educational college, Baghdad, Iraq

***Corresponding author:** Bahaajawad82@uomustansiriyah.edu.iq

ORCID: https://orcid.org/0000-0002-9795-3937

ABSTRACT

Patients suffering from renal failure often exhibit severe disturbances of mineral and electrolyte homeostasis, placing a heavy demand on rapid & accurate diagnostic techniques for routine clinical monitoring. In this pilot study, we report the successful application of Laser-Induced Breakdown Spectroscopy (LIBS) to examine hemodialysis effects on blood mineral balance in serum samples from healthy subjects and renal failure patients prior to and post-dialyzer. We proposed a new relative intensity-based spectral method, termed the Intensity Ratio Index (IRI), to analyze differences of calcium (Ca), potassium (K), phosphorus (P), magnesium (Mg), and zinc (Zn) without complex calibration processes.

The main contribution of this work is to demonstrate the viability of LIBS in a fast, less invasive, and cost-effective manner for assessing dialysis efficacy as well as mineral imbalance online. The resulted values were highly different for potassium and phosphorus in pre-dialysis, with effect ratios of around 73.8% & 74.2%, respectively; these parameters suggest serious electrolyte disturbance associated with renal

dysfunction. In contrast, post-dialysis analysis presented partial restoration of mineral homeostasis exclusively for calcium with an improvement ratio around 36%. Additionally, the study validated that LIBS can detect rapid and sensitive relative spectral changes in both major and trace elements. These results suggest great potential for the use of LIBS as an effective clinical diagnostic method for monitoring renal failure and determining hemodialysis effectiveness.

Keywords: Renal failure, Minerals, LIBS technique, Potassium, Calcium, Phosphorus, Magnesium, Zinc

1. Introduction

We define renal failure — especially chronic kidney disease (CKD) — as a major global health challenge of progressive decline in nephron function that destabilizes metabolism. The imbalance of essential minerals and electrolytes, such as calcium (Ca), potassium (K), phosphorus (P), magnesium (Mg), and zinc (Zn) is one of the most critical consequences of renal dysfunction and these elements play vital roles in cellular signaling, neuromuscular activity, and physiological stability. They are widely known to be linked with rising morbidity and mortality, particularly in individuals on haemodialysis where regular assessment of the mineral status is crucial for optimal clinical management.[1-4].

It is very common to use conventional analytical methods, such as inductively coupled plasma mass spectrometry (ICP-MS) or atomic absorption spectroscopy (AAS), to evaluate low concentrations of elements in biological samples. Nonetheless, these approaches often demand significant sample preparation, lab-based facilities and long analysis times, restricting much or all of their use for rapid or real-time clinical surveillance[5-8]. This demand emphasizes the necessity of analytical strategies which allow rapid, accurate and non-invasive monitoring of the mineral status at point-of-care settings[9, 10].

Laser-Induced Breakdown Spectroscopy (LIBS) is a new analytical technique that has been regarded as very promising for both fast elemental analyses in different matrices, including biological ones[11-13]. Advantages of LIBS include the need for minimal sample

preparation, rapid or real-time detection, multi-element capability, and possibility for in situ analysis [14-17]. During the last few years, LIBS has been gradually developed and explored towards biomedical applications, with blood[18-20], tissues and biofluids[13] most notably analysed (demonstrating notable potential for diagnostics/monitoring purposes)[21, 22]. However, direct quantitative analysis by LIBS in complex biological matrices remains problematic because of variations in plasma emission, matrix effects and differences between experimental conditions. As a result, there is still a demand for simplified and robust approaches that can give accurate relative measurements of elemental differences without the need for complete calibrations[23-26]. Here we present a method based on monitoring relative intensities for the assessment of mineral differences in blood serum samples from healthy and renal failure patients prior to and following haemodialysis. A spectral index that is based on emission line intensities relative to one another, rather than on any absolute measure of quantification, is used to trace changes in elemental behavior. The main aim of this work is to evaluate the viability of this method as a rapid and portable dosing device for dialysis monitoring and mineral dysfunction diagnosis in a bedside setting.

2. Materials and Methods

2.1 Sample Collection and Preparation

The blood samples were obtained from three groups of subjects: healthy persons (control group); patients with renal failure before hemodialysis treatment (pre-dialysis), and the same patients after hemodialysis treatment (post dialysis). All samples were handled similarly to avoid differences due to external variables.

Blood samples obtained were placed in standard collection tubes (Figure 1). Sample Centrifugation (Serum Separation) was performed as represented in Figure 2, the sample were centrifuged which properly separates serum phase from whole blood. After centrifugation, the top serum layer was carefully collected and subjected to a LIBS analysis.

Figure 1 :Blood samples collected in standard tubes prior to serum separation.

Figure 2 :Centrifugation process used to separate serum from whole blood samples.

2.2 LIBS Experimental Setup

A Q-switched Nd:YAG laser (1064 nm) was used for all LIBS measurements. The energy of the laser pulse was high enough to produce a stable plasma on the sample surface. Plasma radiation emitted was captured through an optical system which is then guided to a spectrometer in the wavelength range of ~321–741 nm through an optical fiber.

Figure 3 shows a schematic of the LIBS experimental setup and includes the laser source, focusing optics, plasma formation and signal collection system.

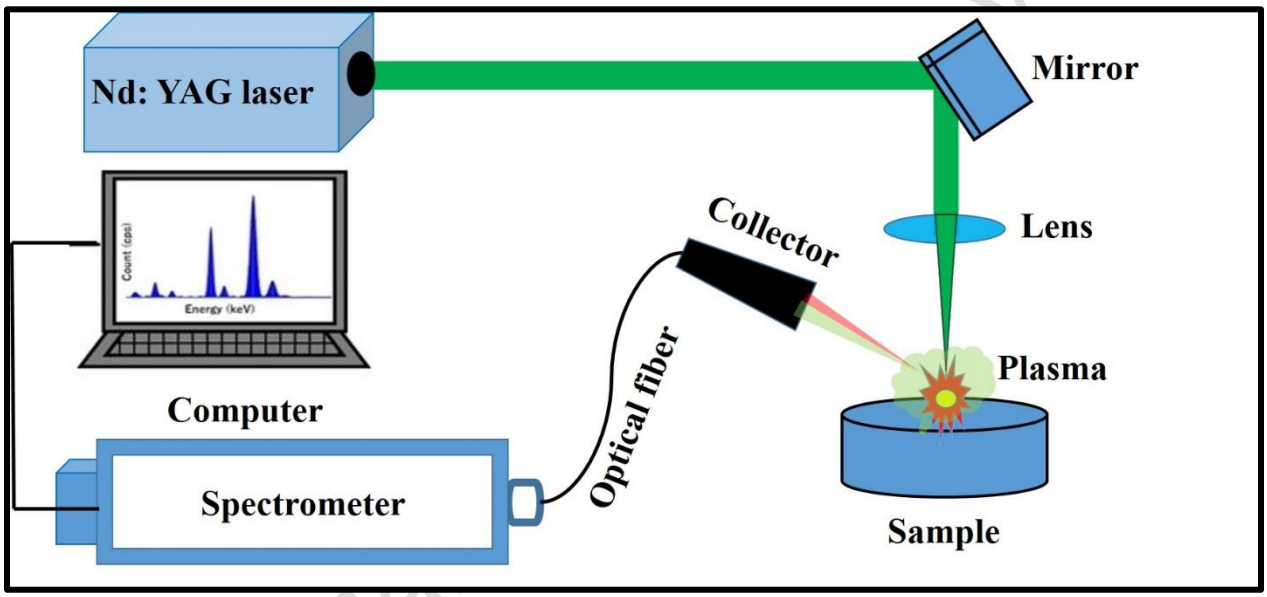

Figure 3 :Schematic diagram of the LIBS experimental setup showing the Nd:YAG laser, focusing optics, plasma generation, and optical emission collection system.

These experimental parameters were optimized for the best signal-to-backdrop ratio. Acquisition parameters of biological samples were set to classic mode: the delay time was within the microsecond range (≈1–2 μs) to achieve continuum suppression, taking the integration time (gate width) – exceeding maximum pulse duration, with overwhelming emission of plasma species.

2.3 Spectral Acquisition

Each spectrum was obtained under the same experimental conditions to maintain sample compatibility. To increase the signal-to-noise ratio (SNR) and to decrease random variations, multiple laser shots (usually 5–10 for each measurement spot) were used. One to two shots of laser before the actual ablative shooting decreased the impact resulting from surface contaminants, also achieving a similar plasma species formation between experiments.

2.4 Spectral Processing

The acquired spectra were processed, using baseline correction and smoothing to reduce the background signal with the idea of enhancing visibility of molecular peaks. No normalization procedure was performed, as spectral comparisons were done on the basis of original recorded intensities to retain the inherent differences within and between sample groups.

2.5 Spectral Line Identification

The emission lines match the spectral wavelength with the NIST Atomic Spectra Database. At most only the brightest and easiest to reproduce emission lines were extracted for analysis. The spectral range as defined (321–741 nm) limits the number of detectable emission lines, such that some like Mg I at 285.12 nm are outside this range and were not fully taken into consideration.

2.6 Intensity Ratio Index (IRI)

What characterizes a relative difference in elemental emission behavior is to derive an intensity-based parameter which we defined as the Intensity Ratio Index (IRI), formulated as follows:

$$\mathrm{IRI} = \frac{\mathrm{I_{min}}}{\mathrm{I_{max}}}$$

Where I_{min} and I_{max} are the minimum and maximum emission intensities for an element, respectively. This parameter is not an absolute concentration but is a relative spectral index mirroring shifts in emission performance across disparate physiological environments.

2.7 Data Interpretation

This is not meant to be an absolute quantitative affair (no external calibration nor CF-LIBS methodology was used). Instead, the IRI parameter is used as a reference for relative differences between healthy and pre-dialysis or post-dialysis samples. Relative intensity ratios minimize the effects of experimental uncertainties, such as laser energy variations, plasma temperature changes and matrix effects, to improve comparability.

Relative changes of elemental behavior — not absolute concentrations — are inferred from differences in emission intensity.

3.Results and Discussion

3.1 LIBS Spectral Analysis

Figures 4–6 show representative LIBS data of the three sample groups (healthy, pre-dialysis and post-dialysis), highlighting significant emission features. Manifest across spectral regions selected.

There are many bright emission lines, as shown by the spectrum of the healthy samples in Fig. 4, corresponding to major elemental lines like Ca, K and P. Another major emission feature, an intensive one at approximately 422.6–422.9 nm with a mineral origin responsible for Ca I (422.67 nm), confirms calcium as a leading element in this serum

matrix. Other peaks at 430 nm, at 559 nm and between 616–617 nm provide additional evidence of calcium transitions.

Some resonant emission lines, for example, Ca I at 422.67 nm, are strongly affected by the phenomenon of line broadening, spectral overlap or local plasma conditions while retaining both apparent intensity and clarity. We therefore interpreted these lines very cautiously based on the overall spectral behaviour rather than purely on an isolated emission feature.

Figure 5. Spectrum samples prior to dialysis Distinct differences in peak intensities, especially in calcium and potassium regions as compared with corresponding healthy samples, are observed. Such alterations could represent the metabolic changes correlated with renal failure. The peak associated with Ca is still found around 422.67 nm, just with different relative intensity, which shows if the plasma conditions or behavior of an element varies or not.

The spectrum after dialysis treatment is shown in Fig. 6. We note that the spectral features are partially restored, especially in the Ca and K emission regions, suggesting a marginal recovery trend after dialysis. This behavior coincides with the conventional correction of electrolyte imbalance in treated patients.

Weak, low-intensity emission features corresponding to trace elements (i.e., Zn near 330–335 nm and 610–636 nm) are also detected. Nonetheless, these signals are redundantly near the threshold of detection and should be understood as absolute elemental spectrometry presence errors.

Importantly, the measured spectral range (321–741 nm) does not include certain emission lines (e.g., Mg I at 285.12 nm), which were excluded from this study as a result. Spectral line assignments were performed (first stage) by matching the wavelengths based on the NIST Atomic Spectra Database. Given the complicated nature of the LIBS plasma and potential line broadening or overlap effects, the given assignments show what we believe to be at least most probable elemental contributions.

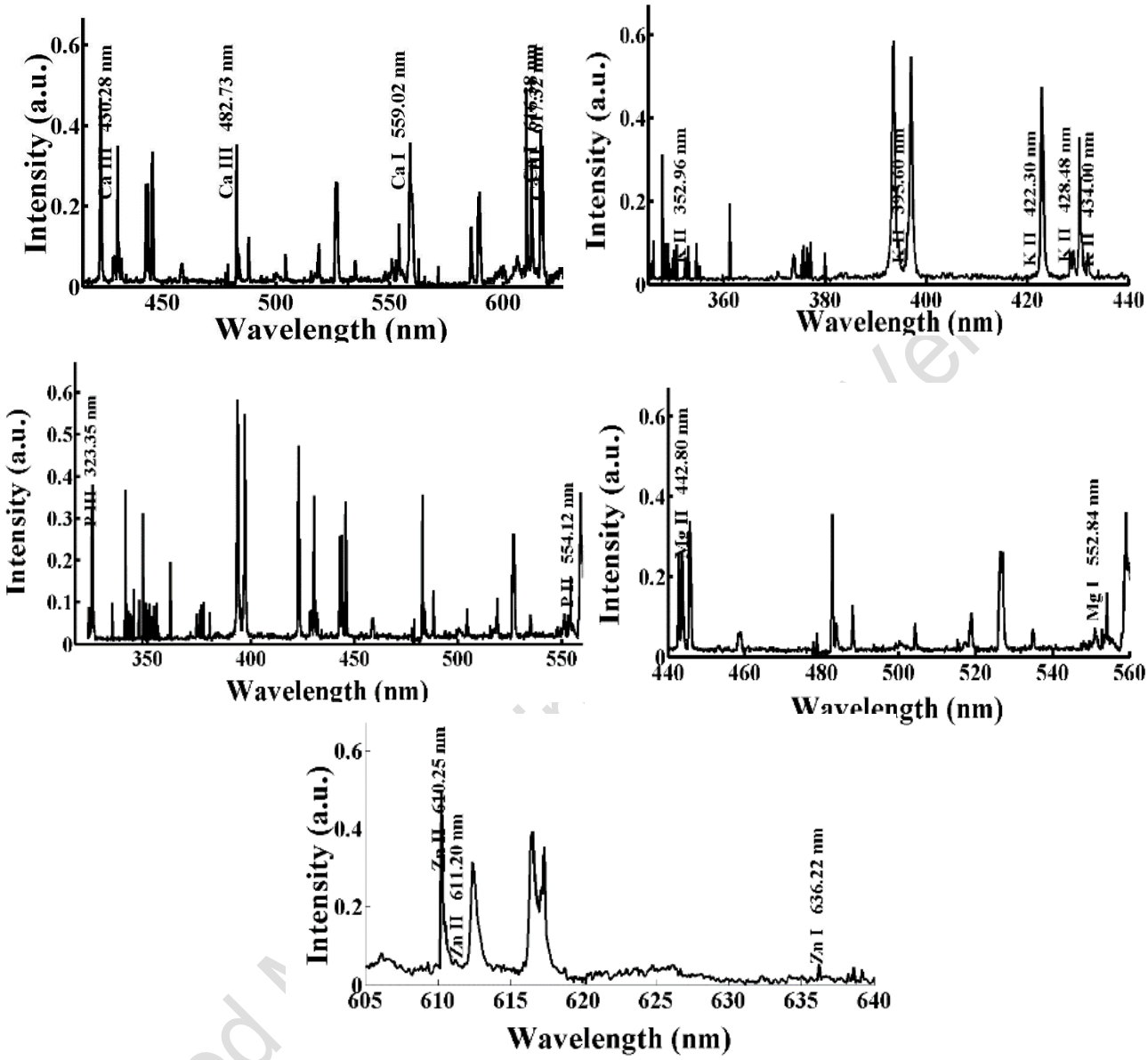

Figure 4: Spectrum of the intact samples.

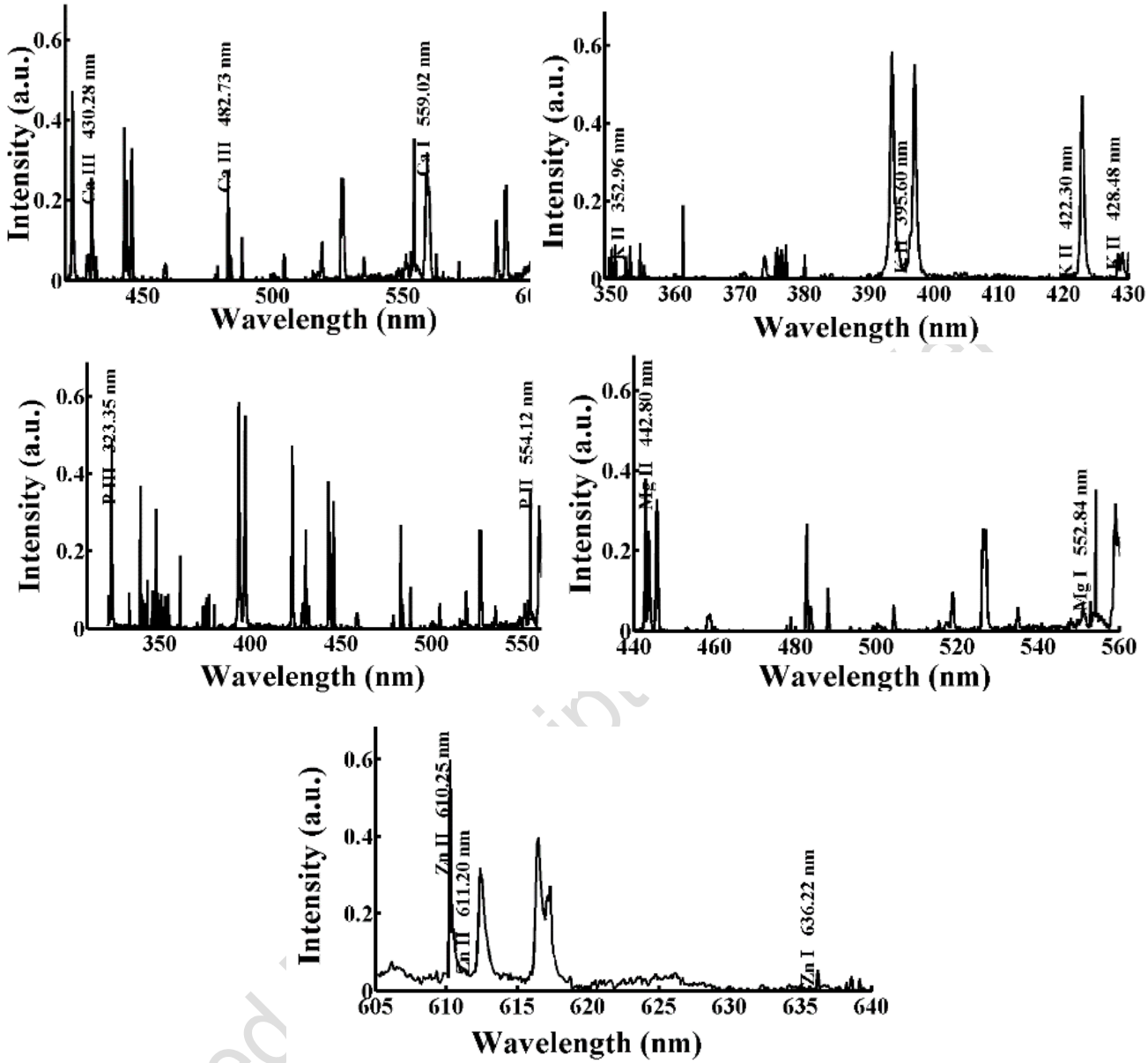

Figure 5: The spectrum of samples before dialysis.

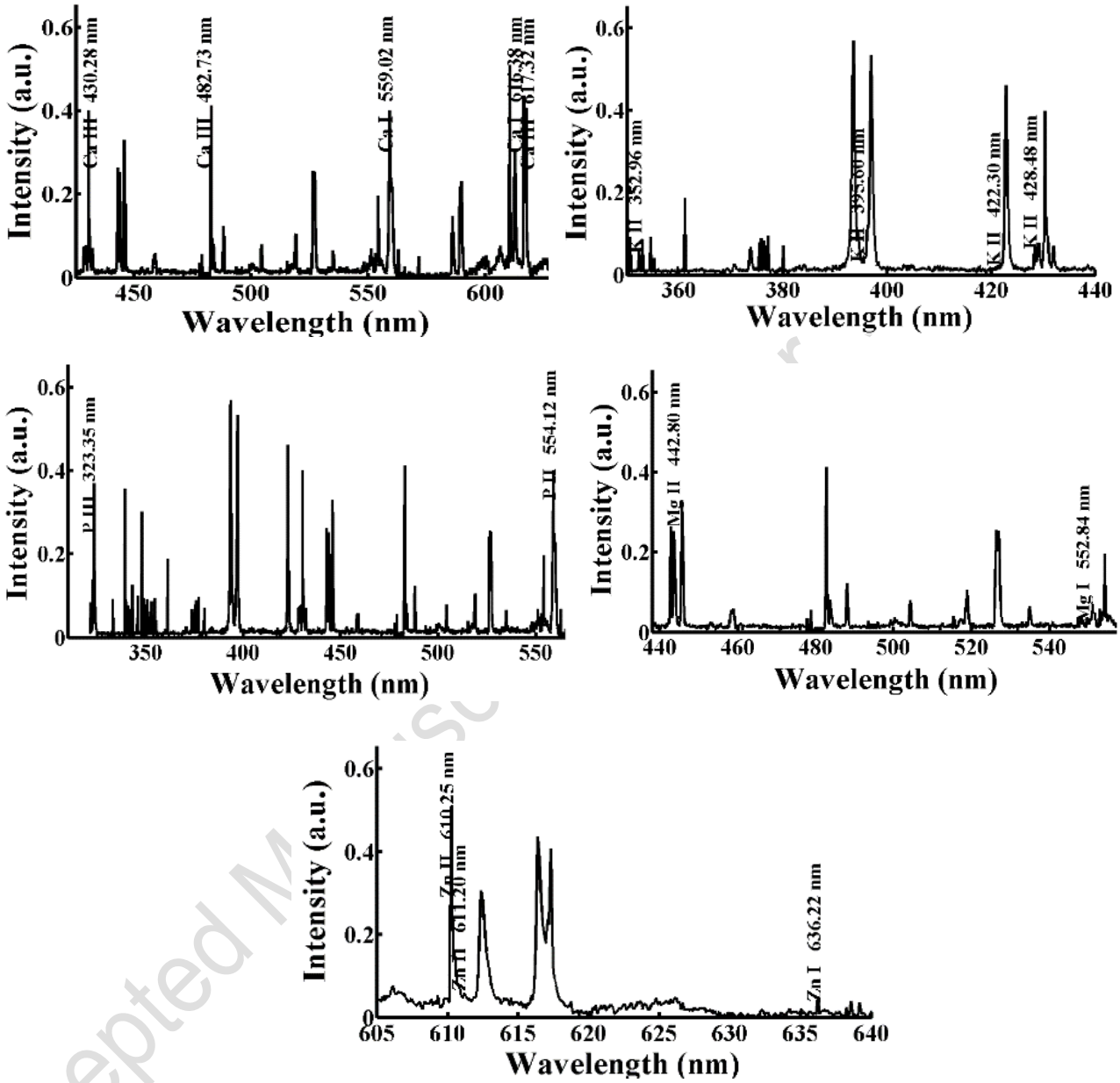

Figure 6: The spectrum of samples after dialysis.

3.2 Spectral Wavelength Analysis and Intensity-Based Evaluation

The corresponding reference values from the NIST Atomic Spectra Database were matched with the identified emission wavelengths extracted from the LIBS spectra. As shown by Tables 1–3, the close agreement of experimental wavelengths with the standard NIST values confirms that spectral line identification is reliable.

Wavelength shifting is small; it can be explained by the fluctuations in local plasma, slight changes in temperature as well as imperfect instrument resolution (a common problem of LIBS measurements).

For the three groups of samples (healthy, pre-dialysis and post-dialysis) the detectable emission lines along with NIST values and measured intensities are summarized in Tables 1–3. These tables are used as a basis for relative comparisons of elemental emission behaviour.

Table 1: LIBS wavelengths for a healthy sample.

Element	Wavelength LIBS	Wavelength NIST	Intensity	Intensity Ratio Index
Ca III	430.2814	430.2804	0.35007	0.938173
Ca III	617.3248	617.3217	0.35025	
Ca III	482.7306	482.7263	0.35336	
Ca I	559.0203	559.012	0.35777	
Ca I	616.3814	616.376	0.37314	
K II	433.9984	434.003	0.0314	0.353843
K II	395.6029	395.61	0.04162	
K II	422.3005	422.297	0.05163	
K II	428.481	428.489	0.07459	
K II	352.9584	352.953	0.08874	
P II	554.1238	554.114	0.15699	0.415757
P III	323.3465	323.3536	0.3776	
Mg I	552.8422	552.8405	0.06772	0.265829
Mg II	442.8026	442.7994	0.25475	
Zn I	636.2213	636.2346	0.05014	0.102345
Zn II	611.1956	611.153	0.05952	
Zn II	610.2532	610.249	0.48991	

Table 2: LIBS wavelengths for renal failure sample.

Element	Wavelength LIBS	Wavelength NIST	Intensity	Intensity Ratio Index
Ca III	430.2814	430.2804	0.2556	0.67249
Ca III	482.7306	482.7263	0.26759	
Ca III	617.3248	617.3217	0.27123	
Ca I	559.0203	559.012	0.31928	
Ca I	616.3814	616.376	0.38008	
K II	395.6029	395.61	0.05155	0.615082
K II	422.3005	422.297	0.06109	
K II	428.481	428.489	0.06373	
K II	352.9584	352.953	0.08381	
P II	554.1238	554.114	0.35272	0.72436
P III	323.3465	323.3536	0.48694	
Mg I	552.8422	552.8405	0.073232	0.191918
Mg II	442.8026	442.7994	0.38158	
Zn I	636.2213	636.2346	0.05375	0.089862
Zn II	611.1956	611.153	0.05724	
Zn II	610.2532	610.249	0.59814	

Table 3: LIBS wavelengths for the infected sample after dialysis.

Element	Wavelength LIBS	Wavelength NIST	Intensity	Intensity Ratio Index
Ca III	430.2814	430.2804	0.39976	0.917259
Ca I	559.0203	559.012	0.40035	
Ca III	617.3248	617.3217	0.40691	
Ca III	482.7306	482.7263	0.41281	
Ca I	616.3814	616.376	0.43582	
K II	395.6029	395.61	0.0408	0.468966
K II	422.3004	422.297	0.05062	
K II	428.481	428.489	0.07313	
K II	352.9584	352.953	0.087	
P II	554.1238	554.114	0.19587	

P III	323.3465	323.3536	0.3702	0.529092
Mg I	552.8422	552.8405	0.05818	0.220981
Mg II	442.8026	442.7994	0.26328	
Zn I	636.2213	636.2346	0.05015	0.098499
Zn II	611.1956	611.153	0.05835	
Zn II	610.2532	610.249	0.50914	

For testing differences within the emission behavior of elements, an intensity-based parameter was used. This parameter is introduced as a relative spectral index based on emission line intensities.

It should be noted that this is not in any way intended to calculate absolute quantitative concentrations. Instead, it is a comparative metric of relative changes in emission behavior for the same experimental circumstances.

3.3 Intensity Ratio Index (IRI) and Elemental Variation

The intensity ratio index (IRI) based on the minimum to maximum emission intensity for each element was derived in order to assess relative changes in elemental emission behavior.

Tables 2 and 3 display the calculated IRI values of Ca, K, P, Mg and Zn for all three sample groups, respectively. Since these values order similar distinctions on the heartbeat exam for sound versus pre-dialysis and post-dialysis conditions.

Calcium (Ca) presents with reduced IRI values in pre-dialysis samples when compared to the healthy group; this is followed by a partial recovery of the IRI after dialysis. This trend is aligned with the disturbance of calcium homeostasis known to occur in renal failure patients. Dialysis treatment reduces potassium imbalance as revealed by the increased relative emission behavior of potassium (K) before and decreased relative emission after treatment.

For phosphorus (P), elevated values are evident in the pre-dialysis samples compared with a partial decrease after dialysis, which is compatible with surmountable phosphate regulation during kidney disease. As trace minerals, there were relatively small variations in magnesium (Mg) and zinc (Zn). Their emission signals are determined to be relatively, not absolutely, quantitative metrics since they may be weakly impacted by plasma conditions and detection limits.

3.4 Effect Ratio (ER) and Improvement Ratio (IR)

For a better assessment of both the impact of renal failure and dialysis treatment, two additional comparative indices, Effect Ratio (ER) and Improvement Ratio (IR), were defined.

The ER is the relative deviation of elemental behavior on pre-dialysis samples away from the healthy group, and the IR is the extent after dialysis of how close to the pre-dialysis condition. Table 4 presents the computed values of ER and IR. The effect of renal failure on an element's intensity and partial correction by dialysis is clearly illustrated by these results.

Calcium has an extreme drop before dialysis and a dramatic recovery pattern post-treatment. Elevated pre-dialysis potassium and phosphorus levels decline after dialysis but may not completely normalize. Zinc is stable in the studied groups, while magnesium has moderate variation.

Table 4: Total concentration, E.R., and I.R. of the studied elements for the three samples.

Element	IRI (Healthy)	IRI (Pre-dialysis)	IRI (Post-dialysis)	Effect Ratio (ER) %	Improvement Ratio (IR) %
Calcium	0.938173	0.67249	0.917259	28.3191906	36.39741855
Potassium	0.353843	0.615082	0.468966	73.82907109	23.75553178
Phosphorus	0.415757	0.72436	0.529092	74.22677189	26.95731404
Magnesium	0.265829	0.191918	0.220981	27.8039642	15.14344668
Zinc	0.102345	0.089862	0.098499	12.1969808	9.611404153

3.5 Discussion of Elemental Behavior

The differences in spectral emission and IRI values observed are attributed to physiology as well as plasma.

Clinically, renal failure alters electrolyte homeostasis by deranging Ca, K and P balance. The LIBS emission behavior observed in this study is a manifestation of these physiological changes. Emission intensity is spectroscopically influenced by plasma temperature, electron density and matrix composition. Thus, the differences found are a result of elemental variation and plasma dynamics combined.

Dialysis restored partial emission behavior, suggesting that electrolyte levels were rebalanced and treatment was effective; however, full normalization may not occur. We caution against the interpretation of weak emission signals, particularly for trace elements such as Zn, which should be carefully interpreted as influenced by detection limits/plasma fluctuations and not necessarily indicative of absence from the particle.

3.6 Methodological Considerations

In particular, the proposed intensity-based approach provides fast and practical means of determining relative elemental variations with minimal or no additional calibration work.

But this does not give true quantitative concentrations. Instead, it becomes a comparative spectroscopic tool for monitoring trends under highly controllable experimental conditions. Although limited by the non-representative nature of each sample site population, similar trends across multiple populations indicate reliability for comparative purposes.

To obtain more quantitative results, the possibilities of calibration-based LIBS methods or combinations with other complementary analytical techniques can be taken into account in future studies.

Conclusions

This study demonstrates mineral imbalances in patients with renal failure using Laser-Induced Breakdown Spectroscopy (LIBS) and demonstrates that LIBS is a

quick, reliable method for monitoring these individuals. Using an approach based on relative spectral variations , we tracked large changes in key elements (Ca, K, P, Mg and Zn) as the hemodialysis proceeded. The obtained results showed a remarkable increment of pre-dialysis potassium and phosphorus with an impressive return to par post-dialysis, statistically supported by the improvement ratios achieved.

Technically, the other advantages of traditional clinical methods are minimal sample preparation and the real-time analytical capabilities of LIBS. Future work will implement machine learning algorithms to improve the prediction accuracy of mineral recovery and extend to a larger cohort for clinical validation. This work highlights the promise of laser-based diagnostics to enable rapid, low-cost feedback for tailored renal management.

Acknowledgment:

The authors would like to thank Mustansiriyah University (www.uomustansiriyah.edu.iq) for its outstanding support in this work.

References

1. Y. C. Hou, C. L. Lu, and K. C. Lu, "Mineral bone disorders in chronic kidney disease," Nephrology 23, 88-94 (2018).
2. L. S. Dalrymple, R. Katz, B. Kestenbaum, M. G. Shlipak, M. J. Sarnak, C. Stehman-Breen, S. Seliger, D. Siscovick, A. B. Newman, and L. Fried, "Chronic kidney disease and the risk of end-stage renal disease versus death," Journal of general internal medicine 26, 379-385 (2011).
3. K. C. Reimer, J. Nadal, H. Meiselbach, M. Schmid, U. T. Schultheiss, F. Kotsis, H. Stockmann, N. Friedrich, M. Nauck, and V. Krane, "Association of mineral and bone biomarkers with adverse cardiovascular outcomes and mortality in the German Chronic Kidney Disease (GCKD) cohort," Bone research 11, 52 (2023).
4. Z. Segal, D. Kalifa, K. Radinsky, B. Ehrenberg, G. Elad, G. Maor, M. Lewis, M. Tibi, L. Korn, and G. Koren, "Machine learning algorithm for early detection of end-stage renal disease," BMC nephrology 21, 518 (2020).
5. A. V. Skalny, T. V. Korobeinikova, M. Aschner, O. V. Baranova, E. G. Barbounis, A. Tsatsakis, and A. A. Tinkov, "Medical application of laser-induced breakdown spectroscopy (LIBS) for assessment of trace element and mineral in biosamples: Laboratory and clinical validity of the method," Journal of Trace Elements in Medicine and Biology 79, 127241 (2023).
6. R. Nader, M. J. Zoory, and H. J. Mohamad, "Proposed novel relative intensity LIBS approach for quantifying heavy metals in sunscreens, compared with AAS," Optical Review 32, 791-801 (2025).

7. R. Nader, M. J. Zoory, and H. J. Mohamad, "Quantitative and qualitative analysis of lip balms in the Iraqi market using LIBS and concentration estimation based on electron density," Journal of Optics (2024).
8. R. Nader, H. J. Mohamad, and M. J. Zoory, "Comparison of Heavy Metals Concentrations in Toothpaste Using Atomic Absorption Analysis and Laser-Induced Breakdown," Journal of Optics (2024).
9. N. Melikechi, H. Ding, S. Rock, and D. Connolly, "Laser-induced breakdown spectroscopy of whole blood and other liquid organic compounds," in *Optical Diagnostics and Sensing VIII*(SPIE2008), pp. 152-158.
10. S. Musazzi, and U. Perini, "Laser-induced breakdown spectroscopy," Springer series in optical sciences 182, E1-E2 (2014).
11. C. S. Nogueira, R. S. Zamboni, S. A. Paschuk, and J. N. Correa, "Assessment of trace elements concentration in cosmetic foundation using X-ray fluorescence technique," Brazilian Journal of Radiation Sciences 12, e2742-e2742 (2024).
12. P. Janovszky, A. Kéri, D. J. Palásti, L. Brunnbauer, F. Domoki, A. Limbeck, and G. Galbács, "Quantitative elemental mapping of biological tissues by laser-induced breakdown spectroscopy using matrix recognition," Scientific Reports 13, 10089 (2023).
13. Z. Zhao, W. Ma, G. Teng, X. Xu, K. Wei, G. Chen, Q. Wang, and W. Xu, "Accurate identification of inflammation in blood based on laser-induced breakdown spectroscopy using chemometric methods," Spectrochimica Acta Part B: Atomic Spectroscopy 202, 106644 (2023).
14. Z. J. Kamil, M. J. Zoory, and H. J. Mohamad, "Estimate of macronutrient concentration in dried flaxseed plants using laser-induced breakdown spectroscopy (LIBS) technique," Journal of Optics 55, 481-487 (2026).
15. N. M. Dbayh, M. J. Zoory, and A. H. Ali, "Thermal Effects in Determination of Plasma Parameters in Fe Metal Model Using LIBS Technique," in *AIP Conference Proceedings*(2025).
16. L. A. Kadhim, A. K. Abdel Hussein, M. J. Zoory, and R. Nader, "Comparison of LIBS and XRF for accurate micronutrient analysis in dried white lemon," Journal of Optics (2025).
17. Z. J. Kamil, M. J. Zoory, and H. J. Mohamad, "LIBS technique for plant mineral ratio analysis and environmental and agricultural importance: a comprehensive review," The European Physical Journal D 78, 27 (2024).
18. I. Sami, M. J. Zoory, and S. H. Lefta, "Quantitative Analysis of Element Calcium Using Laser-Induced Breakdown Spectroscopy for Patients with Chronic Renal Failure," in *AIP Conference Proceedings*(2025).
19. Z. Yue, C. Sun, F. Chen, Y. Zhang, W. Xu, S. Shabbir, L. Zou, W. Lu, W. Wang, and Z. Xie, "Machine learning-based LIBS spectrum analysis of human blood plasma allows ovarian cancer diagnosis," Biomedical optics express 12, 2559-2574 (2021).

20. I. Sami, M. J. Zoory, and S. H. Lefta, "Implementation of laser-induced breakdown spectroscopy (LIBS) technique in evaluating of renal failure in patients with iron (Fe) deficiency," Advancements in Life Sciences 11, 66-71 (2024).
21. W. D. Musyoka, A. H. Kalambuka, D.-M. Alix, and K. K. Amiga, "Rapid diagnosis of malaria by chemometric peak-free LIBS of trace biometals in blood," Scientific Reports 12, 20196 (2022).
22. J. Manrique, P. Garrido, and J. Velasco, "Laser-induced breakdown spectroscopy in biological samples: a review of experiments with soft tissues," Atoms 12, 21 (2024).
23. I. Rehan, M. Khan, K. Rehan, S. Sultana, M. Rehman, R. Muhammad, M. Ikram, and H. Anwar, "Quantitative analysis of Fuller's earth using laser-induced breakdown spectroscopy and inductively coupled plasma/optical emission spectroscopy," Applied Optics 58, 4227-4233 (2019).
24. Z. J. Kamil, M. J. Zoory, and H. J. Mohamad, "Application of a new method to estimate micronutrient concentration percentages in dried celery plants using LIBS and XRF techniques," Journal of Optics (2024).
25. I. Rehan, M. Z. Khan, I. Ali, K. Rehan, S. Sultana, and S. Shah, "Spectroscopic analysis of high protein nigella seeds (Kalonji) using laser-induced breakdown spectroscopy and inductively coupled plasma/optical emission spectroscopy," Applied Physics B 124, 49 (2018).
26. J. Aguilera, and C. Aragón, "Characterization of laser-induced plasmas by emission spectroscopy with curve-of-growth measurements. Part I: temporal evolution of plasma parameters and self-absorption," Spectrochimica Acta Part B: Atomic Spectroscopy 63, 784-792 (2008).